Parity-Violating Potentials for the Torsional Motion of Methanol (CH_3OH) and Its Isotopomers (CD_3OH, $^{13}CH_3OH$, CH_3OD, CH_3OT, CHD_2OH, and CHDTOH)

Robert Berger[a]), **Martin Quack***, **Achim Sieben**, and **Martin Willeke**

Laboratorium für Physikalische Chemie, ETH Hönggerberg, HCI, CH-8093 Zürich
(fax: +41-1-6321021; phone: +41-1-6324421; e-mail: martin@quack.ch)
[a]) Institut für Chemie, Technische Universität Berlin, Strasse des 17. Juni 135, D-10623 Berlin

Dedicated to Professor *Duilio Arigoni* on the occasion of his 75th birthday

We present calculations on the parity-conserving and the parity-violating potentials in several MeOH isotopomers for the torsional motion by the newly developed methods of electroweak quantum chemistry from our group. The absolute magnitudes of the parity-violating potentials for MeOH are small compared to H_2O_2 and C_2H_4, but similar to C_2H_6, which is explained by the high (threefold) symmetry of the torsional top in MeOH and C_2H_6. 'Chiral' and 'achiral' isotopic substitutions in MeOH lead to small changes only, but vibrational averaging is discussed to be important in all these cases. Simple isotopic sum rules are derived to explain and predict the relationships between parity-violating potentials in various conformations and configurations of the several isotopomers investigated. The parity-violating energy difference $\Delta_{pv}E = E_{pv}(R) - E_{pv}(S)$ between the enantiomers of chiral CHDTOH, first synthesized by *Arigoni* and co-workers, is for two conformers *ca.* $-3.66 \cdot 10^{-17}$ and for the third one $+7.32 \cdot 10^{-17}$ hc cm^{-1}. Thus, for $\Delta_{pv}E$, the conformation is more important than the configuration (at the equilibrium geometries, without vibrational averaging). Averaging over torsional tunneling may lead to further cancellation and even smaller values.

1. Introduction. – Among the many facets of research on MeOH, which range from its large-scale industrial production and use as a propellant, requiring its statistical thermodynamics and kinetics of combustion [1], to its prototype role in infrared multiphoton excitation and dissociation [2] and, finally, its high-resolution spectroscopy, intramolecular vibrational redistribution [3], and tunneling dynamics [4], certainly a particularly intriguing result was the synthesis and characterization of the chiral isotopomer CHDTOH by *Arigoni* and co-workers [5][6]. This molecule can also be considered to be one of the simplest representatives of $XOCR_1R_2R_3$ type of molecules, which have been proposed for the possible construction of an absolute molecular clock (using also the antimatter enantiomers [7]). While not of immediate practical use for clockmakers, this proposal is certainly of fundamental, conceptual interest regarding the validity of the CPT theorem (see also [8] for a discussion).

The goal of the present work was somewhat more modest. We examined in a series of calculations parity-violating potentials in several MeOH isotopomers. Parity violation arises from the electroweak interaction and leads to different energies for the two enantiomers of a chiral molecule. We addressed the following questions: *1*) what is the magnitude of parity-violating potentials as a function of torsional angle in a molecule of threefold internal-rotational symmetry compared to similar molecules of lower internal-rotational symmetry; *2*) how does 'achiral' isotopic substitution change

the parity-violating potentials as compared to 'chiral' isotopic substitution; and *3*) can we find a simple isotopic-substitution sum rule to predict at least some of the parity-violating energies without explicit calculation?

We shall answer these questions by making use of new theoretical approaches developed in recent years in our group, which have led us to the striking theoretical discovery of order-of-magnitude increase for parity-violating potentials [9–12] as compared to earlier theoretical calculations [13] (for a recent review, see [14]).

2. Theory. – We have previously described in some detail the parity-conserving potential and tunneling dynamics of MeOH [4]. The parity-conserving electronic potential energy was calculated with the Gaussian 98 program package [15]. The electron correlation was treated by second-order *Møller–Plesset* perturbation theory (with all electrons correlated), and the basis set consisted of 94 contracted *Gaussian* functions, corresponding to triple-zeta quality ((11s6p)/[5s4p] for C- and O-atoms; (5s)/[3s] for H-atoms) augmented by polarization functions: two d functions for C- and O-atoms (d exponents: 1.2 and 0.4 for C, 1.35 and 0.45 for O) and two p for H-atoms (p exponents: 1.5 and 0.5) [16]. We have recently shown that the agreement is excellent between experimental data (IVR dynamics [3] and torsional tunneling dynamics [4][17]) and theoretical results with this basis on the MP2 level of theory. As in [4], the reaction path was calculated as a *Fukui* path [18], starting from the eclipsed transition-state structure and following the mass-weighted steepest descent using the intrinsic-reaction-coordinate (IRC) option of Gaussian 98. Thirty points were calculated for each segment between a first-order saddle point and a minimum, exploiting symmetry to cover the full range of the periodic reaction path.

In *Fig. 1*, the torsional angle τ is defined in the *Newman* projection. The reaction-path coordinate q itself is approximately proportional to τ ($q = 0-3.1\ a_0 u^{1/2}$ corresponds to a counterclockwise rotation of the OH group from $0-120^\circ$). It should be noted that, somewhat dependent upon τ, the C_{3v} point-group symmetry of the CH_3 group is more or less broken for the optimized geometries along the reaction path, mainly by the relaxation of the HCH bond angles and the C–H bond lengths. A better description of the reaction path than $\tau \sim q$ is given by the symmetry-adapted combination of dihedral angles ($q \sim \tau + (\delta_1 - \delta_2)/3$) [4].

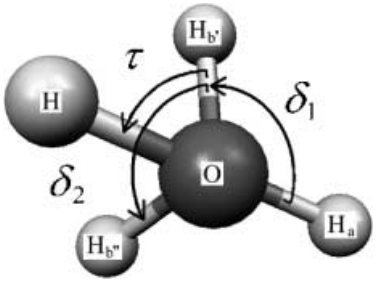

Fig. 1. Newman *projection of MeOH indicating the torsional angle* τ (dihedral angle between the HOC and the $H_{b'}CO$ plane). The angle τ closely follows the reaction coordinate, but relaxation of the CH_3-group bond angles and lengths slightly breaks the C_3 symmetry along τ. The term δ_1 defines the dihedral angle between the planes spanned by $H_{b'}CO$ and COH_a, δ_2 is the corresponding dihedral angle between the planes spanned by $H_{b'}CO$ and $COH_{b''}$, and τ, δ_1, and δ_2 have a counterclockwise orientation.

The parity-violating potentials (V_{pv}) were calculated with our recently described multiconfiguration linear-response (MC-LR) approach to electroweak quantum chemistry [12][19]. Here, we have restricted ourselves to the random phase approximation limit (RPA), as implemented in the *Dalton* program package [20], which has been modified to include parity violation by the approach of [12]. The approximate parity-violating Hamiltonian in SI units reads as:

$$\hat{H}_{pv} = \frac{G_F}{2m_e c\sqrt{2}} \sum_{i=1}^{n} \sum_{A=1}^{N} Q_w(A) \left\{ \hat{\vec{p}}_i \cdot \hat{\vec{s}}_i, \delta^3(\vec{r}_i - \vec{r}_A) \right\}_+ \quad (1)$$

with the *Fermi* constant $G_F = 2.22254 \cdot 10^{-14}\, E_h a_0^3$, m_e being the electron rest mass and c the speed of light in vacuum. The electron index is denoted by i, and $\vec{p}_i$ and $\vec{s}_j$ are the electron's momentum and spin operators, respectively, while $\vec{r}_i$ denotes its position. The term $\vec{r}_A$ is the position vector of nucleus A, and $\delta^3(x)$ represents the three-dimensional *Dirac* delta distribution, and $\{...\}_+$, the anticommutator. The strength of the resulting effect is related to the number of protons (Z_A) and neutrons (N_A) in the corresponding nucleus A, which enter the Hamiltonian *via* the electroweak charge:

$$Q_w = Z_A(1 - 4\sin^2\theta_w) - N_A \quad (2)$$

with the *Weinberg* angle θ_w. Within the RPA method, we used different basis sets abbreviated with roman numbers, as indicated in *Table 1*.

Table 1. *Roman Numeral as Shorthand for Various Basis Sets in RPA Calculations*

Number	Basis set
I	6-31 G(d,p)
II	6-311G(d,p)
III	6-311 ++ G(d,p)
IV	cc-pVDZ
V	cc-pVTZ
VI	aug-cc-pVDZ

3. Results and Discussion. – We used the geometries along the IRC path of CH_3OH for all isotopomers investigated. Thus, we neglected the isotope dependence of the IRC path. This was reasonable because the geometries along the various IRC paths of the isotopes considered are quite similar. In general, V_{pv} depends significantly on the molecular geometry. To visualize the influence of different paths on V_{pv}, we calculated for CH_3OH the V_{pv} potential along a torsional path, where the CH_3 group was forced to C_{3v} symmetry, which yields clearly different geometries compared with the ones from the IRC path. In a comparison of these two paths, we found that the maximal values for V_{pv} differ by up to $4 \cdot 10^{-16}\,cm^{-1}$ (50%), which is quantitatively important, but would not change the qualitative conclusions.

3.1. *CH_3OH*. To compare the results for different basis sets, we listed in the first row of *Table 2* the calculated $V_{pv}(q)$ values for CH_3OH at $q = 0.75 a_0 u^{1/2}$ ($\tau \simeq 30.2°$; see *Fig. 2* for the complete potential functions). At this point, which is rather far away from the equilibrium geometry ($q_{eq} = 1.55 a_0 u^{1/2}$), $|V_{pv}|$ approximately reaches its maximum value for all basis sets investigated. These values are in the range of $7 - 13 \cdot 10^{-16}$ cm^{-1}, which is in agreement with the result of an earlier calculation of the normal isotopomer [21], where a maximum value of $11.4 \cdot 10^{-16}$ cm^{-1} for $\tau = 30°$ was reported (RPA method with slightly different double-zeta basis set and with neglect of the two-electron term of the spin-orbit-coupling operator). The result of *Faglioni* and *Lazzaretti* [21], however, is not based on the IRC geometry employed herein and can, therefore, not be quantitatively compared with our results. Our calculations with basis sets of triple-zeta quality (II, III and V) always gave rise to somewhat larger values compared with basis sets of double-zeta quality (I, IV, VI). The differences between the results of double- and triple-zeta basis sets I and II were larger than those between IV and V. Additional diffuse functions gave only slight corrections (II compared with III, and IV with VI),

Table 2. V_{pv} [hc cm^{-1}] *Values Corresponding to Maximum Absolute Values as a Function of the Torsional Angle τ Calculated with Different Basis Sets* (as indicated in *Table 1*) *at* $q = 0.75 a_0 u^{1/2}$, *which corresponds to* $\tau \approx 30.2°$

	I	II	III	IV	V	VI
CH_3OH	$-7.78 \cdot 10^{-16}$	$-1.23 \cdot 10^{-15}$	$-1.21 \cdot 10^{-15}$	$-9.20 \cdot 10^{-16}$	$-1.30 \cdot 10^{-15}$	$-8.66 \cdot 10^{-16}$
CD_3OH	$-7.76 \cdot 10^{-16}$	$-1.22 \cdot 10^{-15}$	$-1.20 \cdot 10^{-15}$	$-9.17 \cdot 10^{-16}$	$-1.30 \cdot 10^{-15}$	$-8.63 \cdot 10^{-16}$
$^{13}CH_3OH$	$-8.84 \cdot 10^{-16}$	$-1.39 \cdot 10^{-15}$	$-1.36 \cdot 10^{-15}$	$-1.04 \cdot 10^{-15}$	$-1.47 \cdot 10^{-15}$	$-9.80 \cdot 10^{-16}$
CH_3OD	$-7.74 \cdot 10^{-16}$	$-1.22 \cdot 10^{-15}$	$-1.20 \cdot 10^{-15}$	$-9.16 \cdot 10^{-16}$	$-1.30 \cdot 10^{-15}$	$-8.64 \cdot 10^{-16}$
CH_3OT	$-7.71 \cdot 10^{-16}$	$-1.22 \cdot 10^{-15}$	$-1.20 \cdot 10^{-15}$	$-9.11 \cdot 10^{-16}$	$-1.29 \cdot 10^{-15}$	$-8.62 \cdot 10^{-16}$

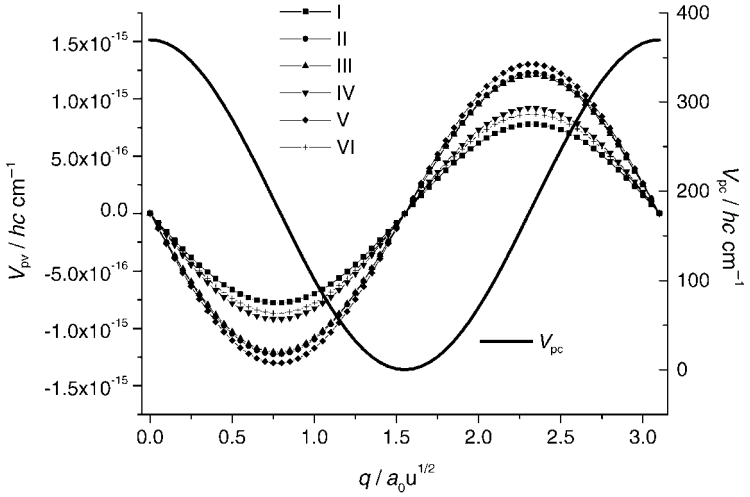

Fig. 2. *Parity-conserving and parity-violating potentials of CH_3OH*. The solid line represents the parity-conserving electronic potential energy V_{pc} along the IRC path following the counterclockwise rotation of the OH group. The reaction coordinate q from 0 to 3.1 $a_0 u^{1/2}$ corresponds to a rotation from $\tau = 0 - 120°$. The different symbols represent the parity-violating potentials V_{pv} obtained with different basis sets as indicated (see *Table 1*).

because they mainly represent the outer electron shell and are, therefore, assumed to be less important for parity violation, since the form of the wave function near the nucleus is important, as can be seen from the parity-violating Hamiltonian (*Eqn. 1*). The antisymmetry of the parity-violating potential around the achiral equilibrium geometry at $q_{eq} = 1.55 a_0 u^{1/2}$ can be nicely seen in *Fig. 2*.

3.2. *Comparison of Isotope Effects in CH_3OH, $^{13}CH_3OH$, CD_3OH, CH_3OD, and CH_3OT.* In *Fig. 3*, the values of $V_{pv}(q)$ for CH_3OH, $^{13}CH_3OH$, CD_3OH, CH_3OD, and CH_3OT are shown for the calculations performed with the aug-cc-pVDZ basis set. Because the molecular symmetry is not changed by the isotope substitutions considered here, the parity-violating potentials remain antisymmetric with respect to torsion around the achiral equilibrium geometry.

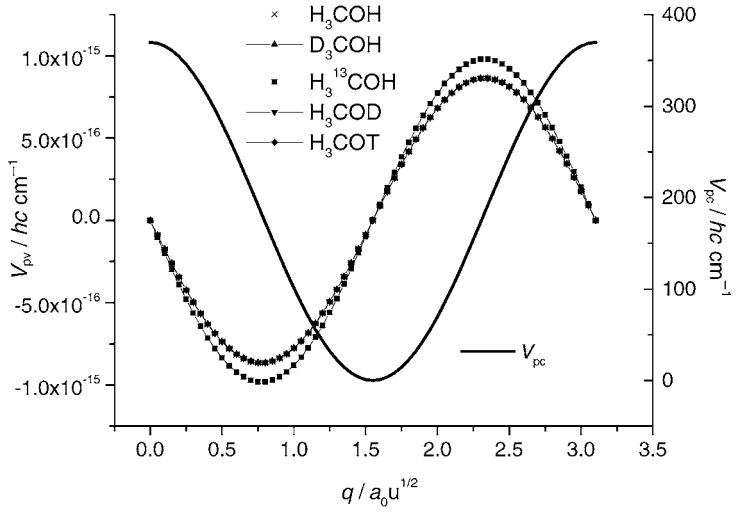

Fig. 3. *Parity-conserving and parity-violating potentials of MeOH and selected isotopomers.* The solid line represents the parity-conserving electronic potential energy along the IRC path for CH_3OH, following the counterclockwise rotation of the OH group. The reaction coordinate q from 0 to 3.1 $a_0 u^{1/2}$ corresponds to a rotation from $\tau = 0 - 120°$. The different symbols represent the parity-violating potentials for a aug-cc-pVDZ basis set. Only the differences between the ^{13}C isotopomer and all the others, which almost coincide, are clearly visible.

The maximum values of $|V_{pv}|$ as a function of torsional angle are listed in *Table 2*. One can see that substituting the H-atoms in CH_3OH with deuterium- (D) or tritium- (T) atoms has only a small effect on V_{pv}. Substituting ^{12}C by ^{13}C, however, enlarges $|V_{pv}|$ by roughly $1 \cdot 10^{-16}$ cm^{-1}, which corresponds to an increase of 10–14%, depending on the basis set. The differences in the parity-violating potentials result, on the one hand, from the different number of neutrons in the nuclei, and, on the other hand, from the shape of the electronic wave function near the nuclei. It should be noted that all isotopomers are described with the same parity-conserving electronic wave function within the *Born–Oppenheimer* approximation. This result demonstrates that not only the number of neutrons (*via* the electroweak charge Q_w in *Eqn. 2*) is crucial for V_{pv}, but also the particular shape of the electronic wave function at a certain nucleus is of importance. For the C-atom with a higher electric charge, the contact-like interaction

between electrons and nucleus is larger than for the H-isotopes, which leads to the well-known larger contribution of this nucleus compared to H-nuclei [10].

3.3. *The Isotopomers CHD_2OH and CHDTOH, and a Simple Sum Rule.* Let us now consider MeOH isotopes with C_S and C_1 symmetry (CHD_2OH, depending on the conformation) and C_1 symmetry ((*R*)-CHDTOH). For these molecules, the V_{pv} potentials for the entire counterclockwise rotation from 0–360° are shown in *Figs. 4* and *5*. In the case of CHD_2OH, we refer to three transition-state structures (**1**, **3**, **5**) and three equilibrium structures (**2**, **4**, **6**), as indicated in *Fig. 4*.

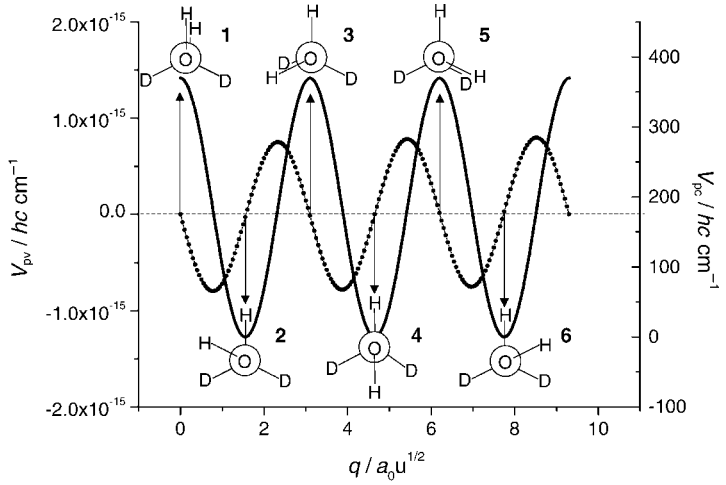

Fig. 4. *Parity-conserving and parity-violating potentials of CHD_2OH.* The solid line represents the parity-conserving electronic potential along the IRC path for CH_3OH, used for CHD_2OH, following the counterclockwise rotation of the OH group. The reaction coordinate q from 0–9.3 $a_0u^{1/2}$ corresponds to a rotation from $\tau = 0–360°$. The circles represent the parity-violating potential for CHD_2OH calculated with a 6-31G(d,p) basis set.

Because of the C_S symmetry of **1** and **4**, the V_{pv} potential vanishes. Employing the helix nomenclature, the rotamers **2** and **3** correspond to the (*M*) configuration. Following the counterclockwise rotation of the OH group from **1** to **4**, we found three local maxima for $|V_{pv}|$. The geometry corresponding to the maximum of $|V_{pv}|$ between **1** and **2** is referred to as **1**–**2** (*etc.*) in *Table 3*. $|V_{pv}|$ at **1**–**2** displayed the largest value of all local maxima. The V_{pv} potential is antisymmetric with respect to the equilibrium geometry of achiral **4**. Since **5** and **6** are the mirror images of **3** and **2**, respectively, the parity-violating potentials, *e.g.*, of **2** and **6**, are different from zero and have the same absolute magnitude, but different signs.

For (*R*)-CHDTOH, we also determined the three minimum and three transition-state geometries, referred to as **7**–**12** in *Fig. 5*. All of these conformers are chiral (C_1 symmetry). The structures **7**, **11**, and **12** correspond to the (*P*), those of **8**, **9**, and **10** to the (*M*)-configuration. The maximal $|V_{pv}|$ values and the corresponding geometries are given in *Table 4*. The largest maximal value of $|V_{pv}|$ is related to the structure **12**–**7**.

Table 3. *Parity-Violating Potential Energies* V_{pv} [*hc* cm^{-1}] *for the CHD$_2$OH Conformers Indicated in* Fig. 4. Structure **1**–**2** refers to that with the maximum absolute value of V_{pv} in the segment going from conformer **1** to **2**. An analogous terminology is used for the other structures.

Structure	I	II	III	IV	V	VI
1	0	0	0	0	0	0
1–**2**	$-7.96\cdot10^{-16}$	$-1.24\cdot10^{-15}$	$-1.22\cdot10^{-15}$	$-9.34\cdot10^{-16}$	$-1.32\cdot10^{-15}$	$-8.76\cdot10^{-16}$
2	$-2.88\cdot10^{-17}$	$-2.42\cdot10^{-17}$	$-2.32\cdot10^{-17}$	$-2.47\cdot10^{-17}$	$-2.67\cdot10^{-17}$	$-1.83\cdot10^{-17}$
2–**3**	$7.51\cdot10^{-16}$	$1.20\cdot10^{-15}$	$1.18\cdot10^{-15}$	$8.95\cdot10^{-16}$	$1.28\cdot10^{-15}$	$8.47\cdot10^{-16}$
3	$-1.45\cdot10^{-17}$	$-1.65\cdot10^{-17}$	$-1.42\cdot10^{-17}$	$-1.44\cdot10^{-17}$	$-1.43\cdot10^{-17}$	$-1.17\cdot10^{-17}$
3–**4**	$-7.82\cdot10^{-16}$	$-1.23\cdot10^{-15}$	$-1.21\cdot10^{-15}$	$-9.24\cdot10^{-16}$	$-1.31\cdot10^{-15}$	$-8.70\cdot10^{-16}$
4	0	0	0	0	0	0
4–**5**	$7.82\cdot10^{-16}$	$1.23\cdot10^{-15}$	$1.21\cdot10^{-15}$	$9.24\cdot10^{-16}$	$1.31\cdot10^{-15}$	$8.70\cdot10^{-16}$
5	$1.45\cdot10^{-17}$	$1.65\cdot10^{-17}$	$1.42\cdot10^{-17}$	$1.44\cdot10^{-17}$	$1.43\cdot10^{-17}$	$1.17\cdot10^{-17}$
5–**6**	$-7.51\cdot10^{-16}$	$-1.20\cdot10^{-15}$	$-1.18\cdot10^{-15}$	$-8.95\cdot10^{-16}$	$-1.28\cdot10^{-15}$	$-8.47\cdot10^{-16}$
6	$2.88\cdot10^{-17}$	$2.42\cdot10^{-17}$	$2.32\cdot10^{-17}$	$2.47\cdot10^{-17}$	$2.67\cdot10^{-17}$	$1.83\cdot10^{-17}$
6–**1**	$7.96\cdot10^{-16}$	$1.24\cdot10^{-15}$	$1.22\cdot10^{-15}$	$9.34\cdot10^{-16}$	$1.32\cdot10^{-15}$	$8.76\cdot10^{-16}$

From the data in *Tables 3* and *4*, one recognizes some relations between the V_{pv} values for different MeOH isotopes (CHDTOH and CHD$_2$OH), as well as for different conformations within one given isotope: $V_{pv}(\mathbf{2}) = -V_{pv}(\mathbf{6}) = V_{pv}(\mathbf{8}) = V_{pv}(\mathbf{10})$; $-V_{pv}(\mathbf{3}) = +V_{pv}(\mathbf{5}) = V_{pv}(\mathbf{11}) = V_{pv}(\mathbf{7})$; $V_{pv}(\mathbf{8}) + V_{pv}(\mathbf{10}) = -V_{pv}(\mathbf{12})$; and $V_{pv}(\mathbf{11}) + V_{pv}(\mathbf{7}) = -V_{pv}(\mathbf{9})$. Some of these relations are defined by symmetry: if a given enantiomer is stabilized due to a parity-violating interaction, its mirror image is destabilized by the same amount of energy. Therefore, $V_{pv}(\mathbf{2}) = -V_{pv}(\mathbf{6})$, and $V_{pv}(\mathbf{3}) = -V_{pv}(\mathbf{5})$, because the corresponding geometries are enantiomeric. We can understand

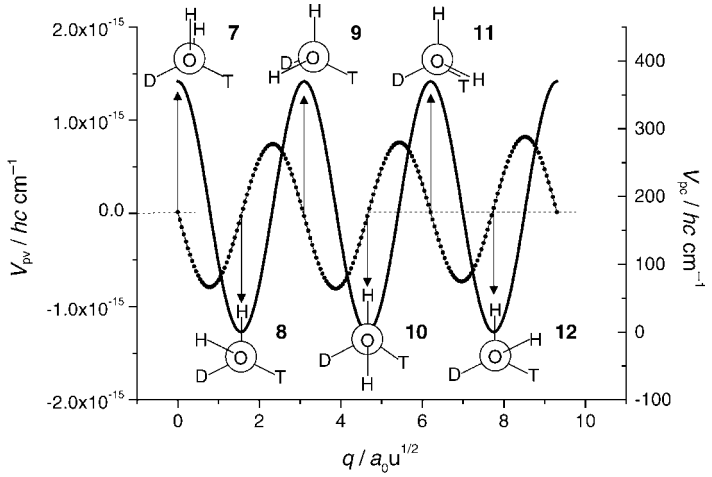

Fig. 5. *Parity-conserving and parity-violating potentials of (*R*)-CHDTOH*. The full line represents the parity-conserving electronic potential along the IRC path for CH_3OH, used as potential for (*R*)-CHDTOH, following the counterclockwise rotation of the OH group. The reaction coordinate q from 0–9.3 $a_0u^{1/2}$ corresponds to a rotation from $\tau = 0–360°$. The circles represent the parity-violating potential for (*R*)-CHDTOH, calculated with the 6-31G(d,p) basis set.

Table 4. *Parity-Violating Potential Energies* V_{pv} [hc cm^{-1}] *for the (*R*)-CHDTOH Conformers Indicated in* Fig. 5. Terminology analogous to *Table 3*.

Structure	I	II	III	IV	V	VI
7	$1.45\cdot10^{-17}$	$1.65\cdot10^{-17}$	$1.42\cdot10^{-17}$	$1.44\cdot10^{-17}$	$1.43\cdot10^{-17}$	$1.17\cdot10^{-17}$
7–8	$-7.90\cdot10^{-16}$	$-1.21\cdot10^{-15}$	$-1.23\cdot10^{-15}$	$-9.27\cdot10^{-16}$	$-1.31\cdot10^{-15}$	$-8.70\cdot10^{-16}$
8	$-2.88\cdot10^{-17}$	$-2.42\cdot10^{-17}$	$-2.32\cdot10^{-17}$	$-2.47\cdot10^{-17}$	$-2.67\cdot10^{-17}$	$-1.83\cdot10^{-17}$
8–9	$7.45\cdot10^{-16}$	$1.19\cdot10^{-15}$	$1.18\cdot10^{-15}$	$8.88\cdot10^{-16}$	$1.27\cdot10^{-15}$	$8.41\cdot10^{-16}$
9	$-2.90\cdot10^{-17}$	$-3.31\cdot10^{-17}$	$-2.85\cdot10^{-17}$	$-2.87\cdot10^{-17}$	$-2.86\cdot10^{-17}$	$-2.34\cdot10^{-17}$
9–10	$-8.06\cdot10^{-16}$	$-1.25\cdot10^{-15}$	$-1.23\cdot10^{-15}$	$-9.45\cdot10^{-16}$	$-1.33\cdot10^{-15}$	$-8.86\cdot10^{-16}$
10	$-2.88\cdot10^{-17}$	$-2.42\cdot10^{-17}$	$-2.32\cdot10^{-17}$	$-2.47\cdot10^{-17}$	$-2.67\cdot10^{-17}$	$-1.83\cdot10^{-17}$
10–11	$7.62\cdot10^{-16}$	$1.21\cdot10^{-15}$	$1.19\cdot10^{-15}$	$9.06\cdot10^{-16}$	$1.29\cdot10^{-15}$	$8.57\cdot10^{-16}$
11	$1.45\cdot10^{-17}$	$1.65\cdot10^{-17}$	$1.42\cdot10^{-17}$	$1.44\cdot10^{-17}$	$1.43\cdot10^{-17}$	$1.17\cdot10^{-17}$
11–12	$-7.31\cdot10^{-16}$	$-1.18\cdot10^{-15}$	$-1.17\cdot10^{-15}$	$-8.78\cdot10^{-16}$	$-1.26\cdot10^{-15}$	$-8.34\cdot10^{-16}$
12	$5.76\cdot10^{-17}$	$4.84\cdot10^{-17}$	$4.64\cdot10^{-17}$	$4.94\cdot10^{-17}$	$5.34\cdot10^{-17}$	$3.66\cdot10^{-17}$
12–7	$8.20\cdot10^{-16}$	$1.26\cdot10^{-15}$	$1.24\cdot10^{-15}$	$9.55\cdot10^{-16}$	$1.34\cdot10^{-15}$	$8.93\cdot10^{-16}$

the remaining relations mentioned above with a simple sum rule. We first divide the parity-violating Hamiltonian into proton- ($\hat{H}_{\mathrm{pv}}^{\mathrm{prot}}$) and neutron- ($\hat{H}_{\mathrm{pv}}^{\mathrm{neu}}$) dependent parts:

$$\begin{aligned}\hat{H}_{\mathrm{pv}} &= \frac{G_{\mathrm{F}}}{2m_{\mathrm{e}}c\sqrt{2}}\sum_{i=1}^{n}\sum_{A=1}^{N}Q_w(A)\left\{\hat{\vec{p}}_i\cdot\hat{\vec{s}}_i,\delta^3(\vec{r}_i-\vec{r}_A)\right\}_+ \\ &= \frac{(1-4\sin^2\theta_w)G_{\mathrm{F}}}{2m_{\mathrm{e}}c\sqrt{2}}\sum_{i=1}^{n}\sum_{A=1}^{N}Z_A\left\{\hat{\vec{p}}_i\cdot\hat{\vec{s}}_i,\delta^3(\vec{r}_i-\vec{r}_A)\right\}_+ \\ &\quad -\frac{G_{\mathrm{F}}}{2m_{\mathrm{e}}c\sqrt{2}}\sum_{i=1}^{n}\sum_{A=1}^{N}N_A\left\{\hat{\vec{p}}_i\cdot\hat{\vec{s}}_i,\delta^3(\vec{r}_i-\vec{r}_A)\right\}_+ = \hat{H}_{\mathrm{pv}}^{\mathrm{prot}}-\hat{H}_{\mathrm{pv}}^{\mathrm{neu}}\end{aligned} \tag{3}$$

Within double-perturbation theory, the parity-violating energy can be calculated with the spin-orbit operator $\hat{H}_{\mathrm{SO}}$ and the parity-violting operator $\hat{H}_{\mathrm{pv}}$:

$$\begin{aligned}V_{\mathrm{pv}} &= 2\mathrm{Re}\left\{\sum_j\frac{\left\langle 0|\hat{H}_{\mathrm{pv}}|\Psi_j\right\rangle\left\langle\Psi_j|\hat{H}_{\mathrm{SO}}|0\right\rangle}{E_0-E_j}\right\} \\ &= 2\mathrm{Re}\left\{\sum_j\frac{\left\langle 0\left|\hat{H}_{\mathrm{pv}}^{\mathrm{prot}}-\hat{H}_{\mathrm{pv}}^{\mathrm{neu}}\right|\Psi_j\right\rangle\left\langle\Psi_j|\hat{H}_{\mathrm{SO}}|0\right\rangle}{E_0-E_j}\right\}\end{aligned} \tag{4}$$

Here, $|0\rangle$ denotes the reference state of interest, *e.g.*, the singlet ground state, E_0 its energy, and $|\Psi_{\mathrm{j}}\rangle$ the jth exited (triplet) state with energy E_{j} [10].

With *Eqns. 3* and *4*, one can evaluate the difference between the parity-violating potential energy for a given molecule (V_{pv}) and that of the same molecule, but with a different isotopic substitution ($V_{\mathrm{pv}}^{\mathrm{iso}}$) at the same geometry. If we now make use of the *Born–Oppenheimer* approximation, both compounds are described by the same electronic wave function. Since the number of protons does not change upon isotopic substitution, the proton-dependent part for V_{pv} and $V_{\mathrm{pv}}^{\mathrm{iso}}$ is identical and cancels out in

$V_{pv} - V_{pv}^{iso}$. However, the neutron dependent part in that difference partly remains, and we get:

$$V_{pv} - V_{pv}^{iso} = 2\mathrm{Re}\left\{ \sum_j \frac{\left\langle 0 \middle| \hat{H}_{pv}^{neu,iso} - \hat{H}_{pv}^{neu} \middle| \Psi_j \right\rangle \left\langle \Psi_j \middle| \hat{H}_{SO} \middle| 0 \right\rangle}{E_0 - E_j} \right\}$$

$$= 2\mathrm{Re}\left\{ \sum_j \frac{\left[\sum_B \left\langle 0 \middle| \frac{G_F}{2m_e c\sqrt{2}} \left(N_B^{iso} - N_B\right) \sum_i \left\{ \hat{\vec{p}}_i \cdot \hat{\vec{s}}_i, \delta^3(\vec{r}_i - \vec{r}_B) \right\}_+ \middle| \Psi_j \right\rangle \right] \left\langle \Psi_j \middle| \hat{H}_{SO} \middle| 0 \right\rangle}{E_0 - E_j} \right\}$$

$$= 2\mathrm{Re}\left\{ \sum_{B,j} \frac{\left(N_B^{iso} - N_B\right) \left\langle 0 \middle| \frac{G_F}{2m_e c\sqrt{2}} \sum_i \left\{ \hat{\vec{p}}_i \cdot \hat{\vec{s}}_i, \delta^3(\vec{r}_i - \vec{r}_B) \right\}_+ \middle| \Psi_j \right\rangle \left\langle \Psi_j \middle| \hat{H}_{SO} \middle| 0 \right\rangle}{E_0 - E_j} \right\}$$

$$= 2\mathrm{Re}\left\{ \sum_B \left(N_B^{iso} - N_B\right) M_{pv}^B \right\} \tag{5}$$

with

$$M_{pv}^B = \sum_j \frac{\left\langle 0 \middle| \frac{G_F}{2m_e c\sqrt{2}} \sum_i \left\{ \hat{\vec{p}}_i \cdot \hat{\vec{s}}_i, \delta^3(\vec{r}_i - \vec{r}_B) \right\}_+ \middle| \Psi_j \right\rangle \left\langle \Psi_j \middle| \hat{H}_{SO} \middle| 0 \right\rangle}{E_0 - E_j} \tag{6}$$

In *Eqn. 5*, $\hat{H}_{pv}^{neu,iso}$ is the neutron-dependent part for the isotopically substituted molecule; N_B and N_B^{iso} are the number of neutrons for the center B, *i.e.*, the isotopic substituted nuclei; $V_{pv} - V_{pv}^{iso}$ is, thus, the sum over all substituted center each of which contributes with the difference of number of neutrons $(N_B^{iso} - N_B)$ multiplied by the factor M_{pv}^B. It is now easy to establish relationships between the parity-violating energies of isotopic substituted molecules. In *Figs. 6* and *7*, we visualize how the general sum rule resulting from *Eqn. 5* can be applied to rationalize the equivalences found in *Tables 3* and *4*. In *Figs. 6* and *7*, the V_{pv} values of the corresponding geometries and their various combinations are graphically represented. In the analysis of the expressions, we made use of the vanishing values for V_{pv} for all C_S-symmetric structures. We finally find that $V_{pv}(\mathbf{2}) = V_{pv}(\mathbf{8})$, and $V_{pv}(\mathbf{10}) + V_{pv}(\mathbf{8}) = -V_{pv}(\mathbf{12})$.

With an analogous procedure, we can also derive $V_{pv}(\mathbf{5}) = V_{pv}(\mathbf{11})$, and $V_{pv}(\mathbf{11}) + V_{pv}(\mathbf{7}) = -V_{pv}(\mathbf{9})$. But there are still two equivalences remaining ($V_{pv}(\mathbf{8}) = V_{pv}(\mathbf{10})$, and $V_{pv}(\mathbf{11}) = V_{pv}(\mathbf{7})$), which have to be explained by exploiting further symmetry arguments. With *Eqn. 5*, $V_{pv}(\mathbf{10}) - V_{pv}(\mathbf{8})$, for example, is given as a sum over contributions from nuclei B. In the framework of the *Born–Oppenheimer* approximation, all nuclei for which the electronic wave function remains invariant under S_n operations (C_S for CH_3OH) do not contribute to V_{pv}. This means that, for (*R*)-CHDTOH, the contributions from the H-, C-, and O-atoms in **10**, as well as T-, C-, O-, and H-atoms in the TCO plane in **8**, vanish in the expression for $V_{pv}(\mathbf{10}) - V_{pv}(\mathbf{8})$.

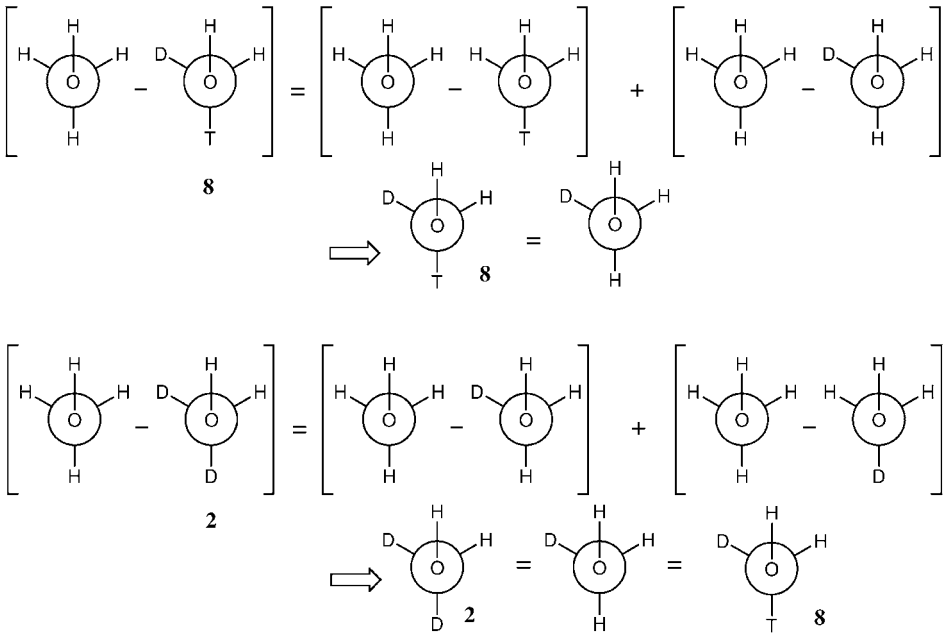

Fig. 6. *Visualization of the sum rule.* Each molecule represents the V_{pv} value related to its geometry. C_S-Symmetric geometries can be neglected due to a vanishing parity-violating potential energy.

Because of the *Born–Oppenheimer* approximation, the factors M_{pv} of the remaining centers adopt the same absolute values, but different signs. We, therefore, get with *Eqn. 5:*

$$V_{pv}(\mathbf{10}) - V_{pv}(\mathbf{8}) = 2\mathrm{Re}\{(2-1)M_{pv} - (1-0)M_{pv}\} = 0 \tag{7}$$

The same procedure can also be applied to the last remaining equivalence, $V_{pv}(\mathbf{11}) - V_{pv}(\mathbf{7}) = 0$. All the relations discussed are actually borne out by the numerical calculations presented in *Tables 3* and *4*.

3.4. *Zero-Point-Energy Effects and Vibrational Averaging of Parity-Violating Potentials.* While we shall not be concerned here with the vibrational-tunneling dynamics [4][17] of MeOH isotopomers, the present analysis, nevertheless, would be incomplete without drawing attention to these effects. From the general magnitude of the parity-violating potentials at the equilibrium geometries of the various conformers as compared to the maximum values as a function of torsional angle, we can directly conclude that vibrational averaging will be significant for the calculation of the parity-violating energy difference of the two stable enantiomers of CHDTOH. Furthermore, the small magnitude of the parity-violating potentials calculated here compared to the tunneling splittings due to torsional motion [4][17] precludes the stabilization of one of the C_1-symmetric enantiomers of CHD_2OH: the energy *eigenstates* of these isotopomers will have essentially pure parity and will be effectively achiral, except for state mixing with 'accidental' degeneracies of levels of different parity [22].

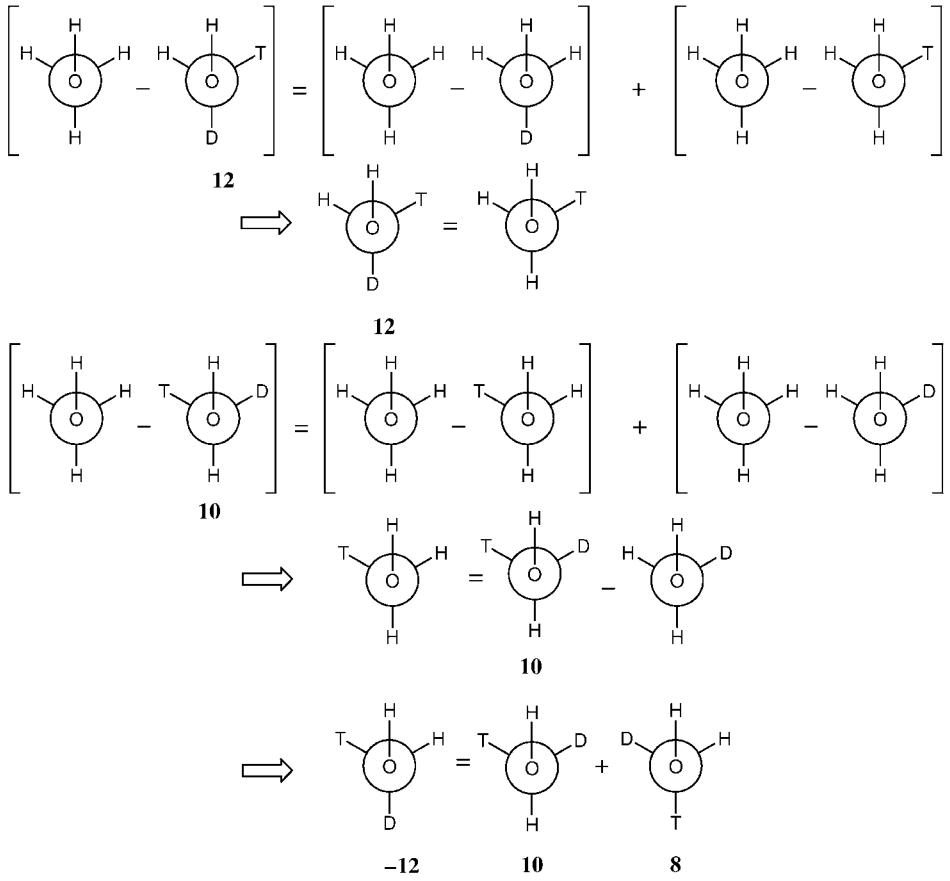

Fig. 7. *Visualization of the sum rule.* For the substitution in the last step, we used the results from *Fig. 6*, taking into account that the parity-violating potential energy for enantiomers only differs in sign.

Finally, we should also point out that, although the *Born–Oppenheimer* pure electronic (parity-conserving) potential shows equivalent degenerate minima for the various conformers of CHD_2OH and CHDTOH, these degeneracies are lifted for two reasons. The first is that the parity-violating potentials lift that degeneracy weakly. The second reason is more important because the zero-point energies defined in the effective lowest quasi-adiabatic channel potentials are much larger and lift these degeneracies as well, except for enantiomeric pairs of molecules, where, for symmetry reasons, only parity violation can lift the degeneracy or equivalence among enantiomers.

4. Conclusions. – Let us now return to the questions formulated in the *Introduction*. The following statements can be made. First, the magnitudes of parity-violating potentials calculated for MeOH can be compared to ethane, where the rotating top has a threefold axis as in CH_3OH, and to ethene and H_2O_2 with a twofold symmetry

(*Table 5*). These molecules are chosen for comparison, as they have similar nuclear charges, *i.e.*, C- and O-nuclei in various combinations. It seems clear that the high internal rotational symmetry favors small 'maximum' values of parity-violating potentials as a function of torsional excursions. Indeed, ethene shows substantially larger parity-violating potentials than methanol, which, nevertheless, contains one O-atom. MeOH and ethane show fairly similar parity-violating potentials, whereas H_2O_2 has the relatively largest parity-violating potentials, which can be related both to its low symmetry and the presence of two O-atoms.

Table 5. *Maximum Values of the Parity-Violating Potential Energy* $|V_{pv,max}(\tau)|$ *for Various Molecules and the Related Torsional Angle* τ *and Symmetry for the Torsional Potential.* For details regarding the remaining structure parameters, see the references cited.

Compound	Symmetry of internal top	τ/°	$\lvert V_{\mathrm{pv,max}} \rvert$ [hc cm^{-1}]
Ethane [10]	threefold	–	*ca.* $4 \cdot 10^{-16}$
Ethane [21]	threefold	30	$12 \cdot 10^{-16}$
Methanol	threefold	30	$7-13 \cdot 10^{-16}$
Methanol [21]	threefold	30	$11 \cdot 10^{-16}$
Ethene [12]	twofold	60–80	$110-290 \cdot 10^{-16}$
H_2O_2 [12]	single (C_1)	40–50	$660-880 \cdot 10^{-16}$

Second, the parity-violating potentials of both chiral and achiral MeOH isotopomers remain small (or even zero by symmetry) at the equilibrium geometries. Thus, vibrational averaging will contribute even more than normally to $\Delta_{\mathrm{pv}}E$ between enantiomers [23–27].

Third, simple isotopic sum rules can, indeed, be found to rationalize (and predict) under exploitation of symmetry relationships the numerical result for parity-violating potentials of certain groups of chiral conformations and configurations of isotopically substituted MeOH molecules, a result that, without doubt, can be extended to other molecules.

Fourth, the parity-violating energy difference $\Delta_{\mathrm{pv}}E = E_{\mathrm{pv}}(R) - E_{\mathrm{pv}}(S)$ between the enantiomers of CHDTOH [5] is for two conformers *ca.* $-3.66 \cdot 10^{-17}$, and for the third one $+7.32 \cdot 10^{-17}$ hc cm^{-1}. Thus, for $\Delta_{\mathrm{pv}}E$, the conformation is more important than the configuration (at the equilibrium geometries, without vibrational averaging). Averaging over torsional tunneling may lead to further cancellation and even smaller values.

Many years of scientific friendship and discussions with *Duilio Arigoni* are gratefully acknowledged. We enjoyed help from and discussions with *Michael Gottselig* and *Jürgen Stohner*. Our work is supported financially by the *Swiss National Science Foundation* and by the ETH Zürich, including C4, CSCS, and AGS. *R. B.* acknowledges financial support by the *Volkswagen Stiftung*.

REFERENCES

[1] W. Tsang, *J. Phys. Chem. Ref. Data* **1987**, *16*, 471, and refs. cit. therein.
[2] O. V. Boyarkin, T. R. Rizzo, D. S. Rueda, M. Quack, G. Seyfang, *J. Chem. Phys.* **2002**, *117*, 9793, and refs. cit. therein.
[3] M. Quack, M. Willeke, *J. Chem. Phys.* **1999**, *110*, 11958.
[4] B. Fehrensen, D. Luckhaus, M. Quack, M. Willeke, T. R. Rizzo, *J. Chem. Phys.* **2003**, *119*, 5534.
[5] D. Arigoni, *Top. Stereochem.* **1969**, *4*, 127.
[6] J. Lüthy, J. Retey, D. Arigoni, *Nature* (London) **1969**, *221*, 1213.

[7] M. Quack, *Nova Acta Leopoldina* **1999**, *81*, 137.
[8] M. Quack, in 'Femtosecond Chemistry', Eds. J. Manz, L. Woeste, VCH, Weinheim, 1994, Chapt. 27, p. 781.
[9] A. Bakasov, T.-K. Ha, M. Quack, in 'Proceedings of the 4th Trieste Conference (1995), Chemical Evolution: Physics of the Origin and Evolution of Life', Eds. J. Chela-Flores, F. Raulin, Kluwer Academic Publishers, Dordrecht, 1996, p. 287.
[10] A. Bakasov, T.-K. Ha, M. Quack, *J. Chem. Phys.* **1998**, *109*, 7263.
[11] A. Bakasov, M. Quack, *Chem. Phys. Lett.* **1999**, *303*, 547.
[12] R. Berger, M. Quack, *J. Chem. Phys.* **2000**, *112*, 3148.
[13] R. A. Hegstrom, D. W. Rein, P. G. H. Sandars, *J. Chem. Phys.* **1980**, *73*, 2329.
[14] M Quack, *Angew. Chem., Int. Ed.* **2002**, *41*, 4618.
[15] M. J. Frisch, G. W. Trucks, H. B. Schlegel, G. E. Scuseria, M. A. Robb, J. R. Cheeseman, V. G. Zakrzewski, J. A. Montgomery Jr., R. E. Stratmann, J. C. Burant, S. Dapprich, J. M. Millam, A. D. Daniels, K. N. Kudin, M. C. Strain, O. Farkas, J. Tomasi, V. Barone, M. Cossi, R. Cammi, B. Mennucci, C. Pomelli, C. Adamo, S. Clifford, J. Ochterski, G. A. Petersson, P. Y. Ayala, Q. Cui, K. Morokuma, P. Salvador, J. J. Dannenberg, D. K. Malick, A. D. Rabuck, K. Raghavachari, J. B. Foresman, J. Cioslowski, J. V. Ortiz, A. G. Baboul, B. B. Stefanov, G. Liu, A. Liashenko, P. Piskorz, I. Komaromi, R. Gomperts, R. L. Martin, D. J. Fox, T. Keith, M. A. Al-Laham, C. Y. Peng, A. Nanayakkara, M. Challacombe, P. M. W. Gill, B. Johnson, W. Chen, M. W. Wong, J. L. Andres, C. Gonzalez, M. Head-Gordon, E. S. Replogle, J. A. Pople, Gaussian 98, Rev. A.11.1, Gaussian Inc., Pittsburgh PA, 2001.
[16] T. H. Dunning Jr., L. B. Harding, A. F. Wagner, G. C. Schatz, J. M. Bowman, *Science* **1988**, *240*, 453.
[17] D. Luckhaus, M. Quack, M. Willeke, to be published.
[18] K. Fukui, *J. Phys. Chem.* **1970**, *74*, 4161.
[19] R. Berger, M. Quack, G. Tschumper, *Helv. Chim. Acta* **2000**, *83*, 1919.
[20] T. Helgaker, H. J. Jensen, P. Jørgensen, J. Olsen, K. Ruud, H. Ågren, T. Andersen, K. L. Bak, V. Bakken, O. Christiansen, P. Dahle, E. K. Dalskov, T. Enevoldsen, B. Fernandez, H. Heiberg, H. Hettema, D. Jonsson, S. Kirpekar, R. Kobayashi, H. Koch, K. V. Mikkelsen, P. Norman, M. J. Packer, T. Saue, P. R. Taylor, O. Vahtras, Dalton: an electronic structure program, Release 1.0 edn., 1997.
[21] F. Faglioni, P. Lazzeretti, *Phys. Rev. E* **2002**, *65*, 011904.
[22] M. Quack, *J. Chem. Phys.* **1985**, *82*, 3277.
[23] M. Quack, J. Stohner, *Phys. Rev. Lett.* **2000**, *84*, 3807.
[24] M. Quack, J. Stohner, *Z. Phys. Chem. (Oldenburg)* **2000**, *214*, 675.
[25] M. Quack, J. Stohner, *Chirality* **2001**, *13*, 745.
[26] M. Quack, J. Stohner, *J. Chem. Phys.* **2003**, *119*, 11228.
[27] R. Berger, A. Sieben, M. Quack, M. Willeke, to be published.

Received September 1, 2003